# Page Proof Instructions and Queries

**Journal Title:** Journal of Mechanical Engineering Science, Proceedings of the Institution of Mechanical Engineers Part C [PIC]

**Article Number:** 614599

Greetings, and thank you for publishing with SAGE. We have prepared this page proof for your review. Please respond to each of the below queries by digitally marking this PDF using Adobe Reader.

Click "Comment" in the upper right corner of Adobe Reader to access the mark-up tools as follows:

For textual edits, please use the "Annotations" tools. Please refrain from using the two tools crossed out below, as data loss can occur when using these tools.

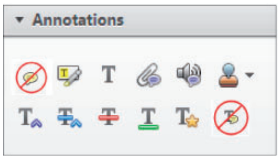


For formatting requests, questions, or other complicated changes, please insert a comment using "Drawing Markups."


Detailed annotation guidelines can be viewed at: http://www.sagepub.com/repository/binaries/pdfs/AnnotationGuidelines.pdf
Adobe Reader can be downloaded (free) at: http://www.adobe.com/products/reader.html.

| No. | Query |
| --- | --- |
| | Please confirm that all author information, including names, affiliations, sequence, and contact details, is correct. |
| | Please review the entire document for typographical errors, mathematical errors, and any other necessary corrections; check headings, tables, and figures. |
| | Please confirm that the Funding and Conflict of Interest statements are accurate. |
| | Please ensure that you have obtained and enclosed all necessary permissions for the reproduction of artistic works, (e.g. illustrations, photographs, charts, maps, other visual material, etc.) not owned by yourself. Please refer to your publishing agreement for further information. |
| | Please note that this proof represents your final opportunity to review your article prior to publication, so please do send all of your changes now. |
| AQ: 1 | Please provide venue of the proceedings for refs [6,7,8,9,11,15] |

Original Article

Proc IMechE Part C:
J Mechanical Engineering Science
0(0) 1–8

DOI: 10.1177/0954406215614599
pic.sagepub.com

# On the comparison between displacement modal testing and strain modal testing

**Emiliano Mucchi**

**Abstract**

The conventional modal testing (referred to as displacement modal testing (DMT)) is based on measurement of displacement, velocity or acceleration as well as excitation force. Though there exits an enormous literature with regard to DMT, on the contrary, a few papers address modal testing based on strain gauges or strain sensor (referred to as strain modal testing (SMT)). The main reason for this scenario is due to practical problems in the use of strain gauges as calibration procedure, ground loop sensitivity are not adequate at high frequency, bonding quality. In this work, a novel piezoelectric strain sensor is used for SMT. In this study it is demonstrated that this sensor overcomes the practical drawbacks related to the use of strain gauges. Thus, SMT based on piezoelectric strain sensors can be a valid alternative to DMT which is usually based on accelerometers. Comparisons between the modal testing results concerning brackets with different constraint conditions using both accelerometers and strain sensors are given in terms of modal parameters, highlighting their pros and cons.

**Keywords**

Experimental modal analysis, strain modal analysis, strain sensor

Date received: 10 February 2015; accepted: 2 October 2015

## Introduction

The conventional modal testing, hereafter referred to as displacement modal testing (DMT) is based on receptance, mobility or inertance measurement, i.e. it is based on measurement of displacement, velocity or acceleration as well as excitation force. An enormous literature regarding the DMT has been published in the Proceedings of the International Modal Analysis Conference (IMAC) and among them, the works of Ewins[1] and Heylen et al.[2] requires a special mention. On the contrary, few papers address modal testing based on strain gauges or strain sensor,[3–12] hereafter referred to as strain modal testing (SMT). As also stated in Bernasconi and Ewins,[3] "this is surprising because mode shapes or displacement eigenfunction, while representing important intermediate results, are normally not the final end products in most structural integrity evaluations. Indeed, strains and stresses are the prime parameters of interest in structural systems which must survive severe dynamics load, i.e. those which are vulnerable to fatigue." The reasons for this *apparent* surprising scenario could be found in Bernasconi and Ewins,[3,4] and Vari and Heyns[10] in which a critical review of the DMT with respect to the SMT based on strain gauges has highlighted the main pros and cons. SMT based on strain gauges presents several drawbacks that strongly reduce its applicability. Main drawbacks are not related to lack of knowledge of strain associated with a mode (eigenvector), but in the practical use of strain gauges. Proper calibration procedure, ground loop, sensitivity not adequate at high frequency due to the lower deformation amplitude and bonding quality (phase delay or amplitude loss can be induced by inadequate bonding) are the major issues in strain gauge measurements.

These are the main reasons related to the disuse of strain sensor for modal analysis. On the contrary, strain sensors are largely used in condition monitoring of mechanical systems for determining wear or degradation of equipment or tools. For example, strain sensors are used for the condition monitoring of the quality of the welding process.[13] It has to be underlined that the strain sensors suitable for condition monitoring or quality control have robust packaging

Engineering Department in Ferrara, Università degli studi di Ferrara, Ferrara, Italy

**Corresponding author:**
Emiliano Mucchi, Engineering Department in Ferrara, Università degli studi di Ferrara, Via Saragat, Ferrara1 – 44100, Italy.
Email: emiliano.mucchi@unife.it

for harsh industrial environments and large dimensions (generally $5 \times 20 \times 15\,\text{mm}^3$) leading to relatively high weight. Thus, they are not suitable for applications in experimental modal analyses (EMA) of lightweight structures or mechanical systems, because of the mass loading effect. Mass loading is the effect caused by adding an extra mass to a dynamic structure. The aim of any measurement is to measure the response of a system as if the measurement equipment is not present. By adding a mass to a dynamic structure, the dynamic behaviour of the structure will change. It is important to minimise this change to ensure the highest quality measurement. Usually, it is recommended to keep the ratio of mass of the item under test to the mass of the sensor below 10:1.[1]

Recently, a novel miniaturised piezoelectric transducer (model PCB 740B02) has been manufactured. It is an integrated electronics piezo electric (IEPE) transducer. It will be demonstrated in the paper that this sensor overcomes the practical drawbacks related to the use of strain gauges. Thus, SMT based on piezoelectric strain sensors can be a valid alternative to DMT, which is usually based on accelerometers. This strain sensor can be suitable for EMA due to the low weight (0.5 g) and dimensions ($5 \times 1.8 \times 15\,\text{mm}^3$) (see Figure 1). Thus, the paper assesses the effectiveness of such a novel miniaturized sensor for application on experimental modal analysis based on strain measurements (i.e. SMT). For this purpose, an EMA campaign has been carried out on two types of brackets with various constraint conditions (freely-supported and clamped condition). These brackets are used in diesel engines to support various engine components such as gear pumps for steering systems or water pumps. The EMA has been carried out by using both genuine piezoelectric accelerometers as well as the novel strain sensor. Two modal analysis algorithms have been used in order to obtain more reliable results in terms of natural frequencies, mode shapes and damping. Comparisons between the results obtained by the accelerometers and the strain sensors are given, highlighting their pros and cons. To the best of author's knowledge, this study is not present in other literatures.

## Literature background

Strain modal testing and analysis are based on the estimation of modal parameters starting from the expression of the strain transfer function, namely strain frequency response functions (SFRF), i.e. the ratio between strain response and excitation force. In the available literature, two different approaches are proposed for deriving the analytical expression of the SFRF, one based on the spatial differentiation of the receptance (i.e. the frequency response function (FRF) between displacement and force),[7,11] and another based on the continuous formulation of solid elastodynamics.[3,4] In the case of viscous damping, the SFRF matrix assumes the form of[11]

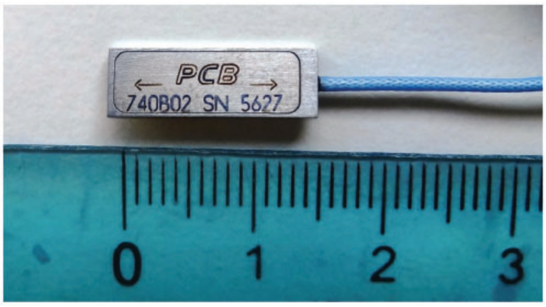


**Figure 1.** Strain sensor.

$$\mathbf{H}^{\varepsilon}(\Omega) = \sum_{r=1}^{N} \frac{\mathbf{\Psi}\mathbf{\Phi}^T}{\omega_r^2 - \Omega^2 + i2\omega_r\Omega\zeta_r} \tag{1}$$

and the receptance matrix, i.e. the FRF matrix in terms of deformation and force is

$$\mathbf{H}^{D}(\Omega) = \sum_{r=1}^{N} \frac{\mathbf{\Phi}\mathbf{\Phi}^T}{\omega_r^2 - \Omega^2 + i2\omega_r\Omega\zeta_r} \tag{2}$$

where $\omega_r$ is the $r$th natural frequency, $i$ the imaginary unit, $\Omega$ the circular frequency, $\zeta_r$ the viscous damping factor for mode $r$, $\mathbf{\Psi}$ the strain modal matrix collecting in each column the strain modal vector $\mathbf{\Psi_r}$, $\mathbf{\Phi}$ the generic element of the displacement modal matrix collecting in each column the displacement modal vector $\mathbf{\Phi}_r$. Note that $\mathbf{\Psi}$=D($\mathbf{\Phi}$) and $\boldsymbol{\varepsilon}$=D($\mathbf{u}$), where $\mathbf{u}$ is the displacement field, $\boldsymbol{\varepsilon}$ the strain field, D the linear spatial differential operator (D: displacement to strain).

It can be noted that the expression of SFRF matrix (equation (1)) and the receptance (equation (2)) are similar. Their difference is that the SFRF matrix is not symmetric and square and thus the reciprocity theorem is not suitable for the SFRF, i.e. the SFRF obtained by the excitation at point $m$ and the response at point $l$ is not equivalent to the response at point $m$ and excitation at point $l$. On the other hand, the receptance matrix is symmetric and it conforms to the theorem. Thus, any column of the SFRF matrix ($\mathbf{H}^{\varepsilon}$) contains information regarding the $r$th strain modal vector (not normalized), while any row contains information regarding the $r$th displacement modal vector (not normalised). Thus, if the response point is fixed and a roving hammer test is considered, the displacement modal vectors are proportional to the numerators of the SFRFs (namely modal constants). Therefore, after the curve fitting procedure, the displacement modal vectors can be estimated. On the other hand, the strain mode shapes can be estimated by exciting the structure in a fixed location, e.g. by a shaker, and measuring the strain at every

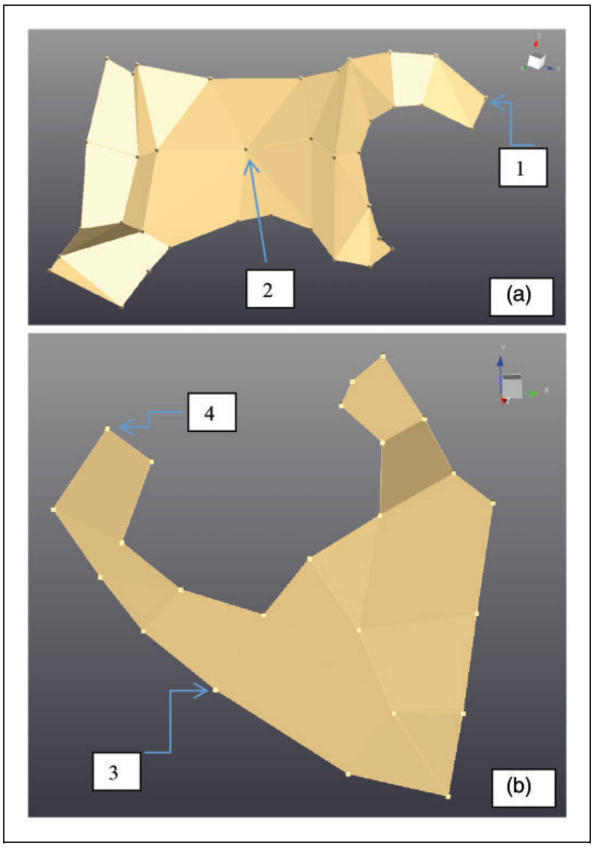


**Figure 2.** Wireframes of the excitation points and position of response points (namely 1,2,3,4) during the EMA of Brackets A and B.

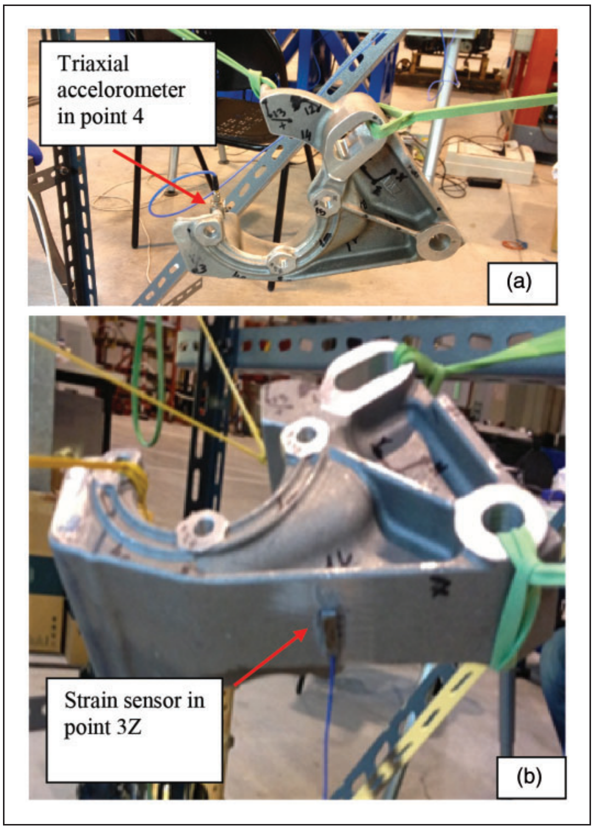


**Figure 3.** Free–free experimental setup for Bracket B with: (a) triaxial accelerometer in point 4 and (b) strain sensor in point 3Z.

response point of interest; the strain modal vectors are then proportional to the numerators of the SFRFs and they can be determined after a curve fitting procedure. Note that the strain modal vector is a surface mode shape since the strain measurements regard surface strains. Normalisation of both displacement modal vector and strain modal vector can be achieved if one line and column are measured and used in the curve fitting procedure. Details are given in Debao et al.[7]

## Experimental setup

The FRFs have been measured for the present modal testing. An impact hammer (PCB 068C04) has been used to excite the different measurement points of the brackets and piezoelectric accelerometers (PCB 356B21, frequency range 1–10,000 Hz) as well as strain sensors (PCB 740B02) have been mounted on the brackets in order to measure the responses. The measurement locations were selected in order to give a suitable spatial resolution for describing the global structural mode shapes. Both excitation and response are measured simultaneously to obtain the inertance, i.e. the FRF between acceleration and force or the SFRFs.

During the modal tests, the excitation moved from one measurement point to another, while the response points were maintained fixed in order to obtain the FRFs (SFRFs) among all the considered points. This procedure allows the estimation of the displacement modal vector both from the DMT based on accelerations and SMT based on strain measurements, as stated in the previous section. Figure 2 depicts the excitation points of the bracket being tested and the position where the responses in terms of acceleration and strain are measured (namely 1 and 2 for Bracket A, 3 and 4 for Bracket B). With the aim of assessing the sensibility of the results to the sensor location, modal tests with strain sensors located in different positions have been carried out, always maintaining the same excitation points. In particular, concerning Bracket A, three different modal tests have been carried out: first by locating the accelerometer in point 1X (i.e. point 1 – direction $X$), second by locating the strain sensor in point 1X and the third by locating the strain sensor in point 2Y. Concerning Bracket B, four different modal tests have been carried out: the first by locating a triaxial accelerometer in point 4 (thus, measuring directions $X$, $Y$, $Z$), the second by locating three strain sensors in point 4Y, 3Z and 3X, the third by locating a strain sensor in point 3Z and the fourth by locating the strain sensor in point 3X (see also Figure 3). The signals were acquired by using sampling frequency and frequency resolution according to the type of brackets and the kind of constrain condition.

The method used for mounting the strain sensor on the test surface is direct adhesive mounting with a quick-bonding gel, as for accelerometers. The surface should be flat with a minimum surface finish of 16 μm. The adhesive layer must be thin and uniform since excessive amounts of adhesive may affect the response of the transducer.

The brackets were tested in two different kinds of constraint conditions. Soft bungee cords were used to suspend the brackets in order to approximate the freely-supported condition (Tables 1 and 2). The brackets on the clamped conditions were analyzed by screwing them to their engine block as in the actual condition (Tables 1 and 2).[14]

## Results and discussion

Once the experimental modal tests and analyses of the brackets have been performed, natural frequencies, modal damping and mode shapes are available for all modes in the frequency band of analysis, both using the acceleration as well as the strain as response. The natural frequency (fn) and modal damping ($\zeta$) were obtained by averaging the values coming from the least square complex exponential (LSCE)[1,2] method and PolyMAX method.[1,15] In particular, two different modal analysis algorithms have been used in order to increase the robustness of the solution: the LSCE method, which works in the time domain and the frequency domain algorithm PolyMAX. In order to evaluate the effectiveness of the SFRFs based on the piezoelectric strain sensor, the modal parameters (natural frequencies, modal damping and mode shapes) estimated by the accelerometers (that will be taken as reference) are compared with the modal parameters estimated by the strain sensor.

As an example, Figure 4 reports the FRF–sum and SFRF–sum, i.e. the complex sum of FRFs and SFRF of all the measured points for Bracket A in the free–free modal test. The figures clearly present peaks, which define the natural frequencies. It is interesting to note that the SFRF–sum curve is clear, well-defined and easy to understand, in comparison with that related to the accelerometers. Tables 1 and 2 collect the natural frequencies and the modal damping for the brackets being studied. Concerning Bracket A, the difference between the natural frequencies estimated by the accelerations and the strains is always less than 6%, while for Bracket B is less than 5%. Thus, the SFRFs based on strain are very accurate in terms of precision in the natural frequency estimation. Also the comparison between modal damping can be considered satisfactory considering the uncertainties related to damping estimation in experimental tests. The modal assurance criterion (MAC)[1] has been used as a technique to determine the degree of correlation between mode shapes. This method has been applied in this paper in order to quantitatively compare the eigenvectors of the different analyses: MAC values close to one indicate a very good correlation (similar mode shapes), MAC values close to zero indicate that the two modes do not show any correlation (different shapes). Usually, MAC values higher than 0.7 indicate good correlation. Tables 3 to 6 compare the mode shapes in terms of MAC. The MAC values presented in these tables clearly state that the three EMA lead to similar mode shapes, in fact the relative MAC values are always higher than 0.7. Thus, the mode shapes estimated by using strains are accurate as those obtained by the accelerometers.

Further modal tests have been carried out in order to assess the sensibility of the results to the sensor location. It is well known[1] that in genuine modal test carried out with accelerometers, the measurement points should not be located in (or close to) nodal lines. Nodal lines[1] are the lines or zones of zero displacement in a certain mode shape. Therefore, when the system being studied is hit on a point along these nodal lines, the system would not experience any vibration from that mode. This behaviour can be analytically explained considering that the dynamic response of a system is a superposition of several modes. Taking as a reference, equation (2), let us consider point l as a nodal point for the particular mode $r$, therefore element $\phi_{lr}$ of the displacement mode shape matrix $\mathbf{\Phi}$ equals zero and, consequently, element $H_{ml}$ of the FRF matrix is zero for every response point m of the system. Obviously, it is expected that when the modal test is carried out with strain sensors, this rule should be respected. The modal tests hereafter presented and discussed aim at verifying this.

Figure 5 depicts the first two mode shapes regarding Bracket B. It is clear that in the first mode the main displacement regards $Z$ direction, while for the 2nd mode the main displacement occurs on the $XY$ plane. A modal test has been carried out by locating the strain sensor in point 3Z and the results has been compared with the accelerometer results (Table 7). It is interesting to note that the MAC values for the first two modes are very low (0.02 and 0.06). This behaviour can be explained considering the particular shapes of the two modes (Figure 5), where they do not experience any deformation in point 3Z (i.e. point 3 – direction $Z$), even if in point 3 a displacement along the $Z$ direction occur. Thus, it is correct that the strain sensor located in point 3Z cannot capture the deformation regarding those two modes. On the contrary, modes 3 and 4 are correctly captured by the strain sensor since such shapes involve deformation of point 3Z, as can be seen in Figure 6. The reader might consider that the strain sensor can measure deformation and not displacement. Furthermore, Figure 7 depicts the first two modes shapes regarding Bracket A. It is clear that the 1st mode is a torsional mode, while the 2nd mode a torsional/flexural mode.

**Table 1.** Results about Bracket A.

| | Freely-supported | Clamped |
|---|---|---|
| Bracket A | 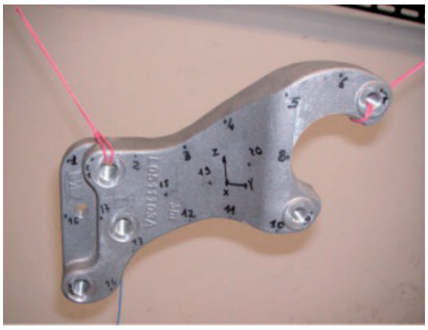 |  |

| | Freely-supported | | | | Clamped | | | |
|---|---|---|---|---|---|---|---|---|
| | Accelerometer | | Strain sensor | | Accelerometer | | Strain sensor | |
| Modal frequencies and damping (mean value of LSCE and PolyMAX methods) | Fn (Hz) | ζ (%) | Fn (Hz) | ζ (%) | Fn (Hz) | ζ (%) | Fn (Hz) | ζ (%) |
| | 1452 | 0.50 | 1510 | 0.32 | 510 | 1.45 | 535 | 1.6 |
| | 2551 | 0.09 | 2661 | 0.1 | 1258 | 0.67 | 1276 | 0.68 |
| | 2965 | 0.13 | 3129 | 0.12 | 1577 | 0.40 | 1586 | 0.5 |
| | 3921 | 0.08 | 3954 | 0.16 | – | – | – | – |
| | 5003 | 0.18 | 5053 | 0.15 | – | – | – | – |

**Table 2.** Results about Bracket B.

| | Freely-supported | Clamped |
|---|---|---|
| Bracket B | 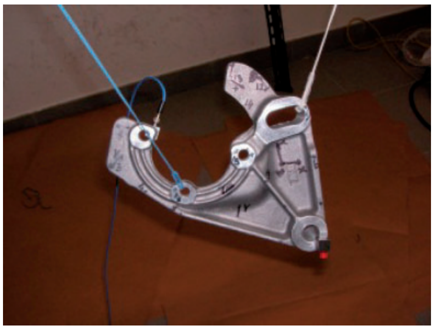 | 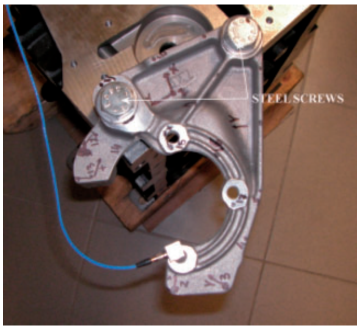 |

| | Freely-supported | | | | Clamped | | | |
|---|---|---|---|---|---|---|---|---|
| | Accelerometer | | Strain sensor | | Accelerometer | | Strain sensor | |
| Modal frequencies and damping (mean value of LSCE and PolyMAX methods) | Fn (Hz) | ζ (%) | Fn (Hz) | ζ (%) | Fn (Hz) | ζ (%) | Fn (Hz) | ζ (%) |
| | 1043 | 0.32 | 1068 | 0.29 | 511 | 0.10 | 525 | 0.22 |
| | 1218 | 0.51 | 1271 | 0.30 | 738 | 0.16 | 760 | 0.23 |
| | 2194 | 0.37 | 2229 | 0.30 | 886 | 0.12 | 887 | 0.1 |
| | 2994 | 0.17 | 3031 | 0.21 | 952 | 0.25 | 953 | 0.14 |
| | 3088 | 0.39 | 3160 | 0.26 | – | – | – | – |

In this case, in point 1X the displacement is high as well the level of deformation. For this reason the MAC values in Tables 3 and 4 are very good.

Thus, in case of acceleration-based modal analysis (i.e. DMT), it is necessary to locate the accelerometers in regions far from nodal lines where the level of displacement is high. On the other hand, in case of strain-based modal analysis (i.e. SMT), it is necessary to locate the strain sensors in regions where the level of deformation is high.

## Concluding remarks

This work addresses the effectiveness of a novel miniaturised piezoelectric strain sensor for application in experimental modal analysis. Comparisons between the results obtained by the genuine modal analysis based on accelerometers and on strain sensors are given, highlighting their pros and cons. From a theoretical standpoint, modal parameters can be achieved both by accelerometer-based data and

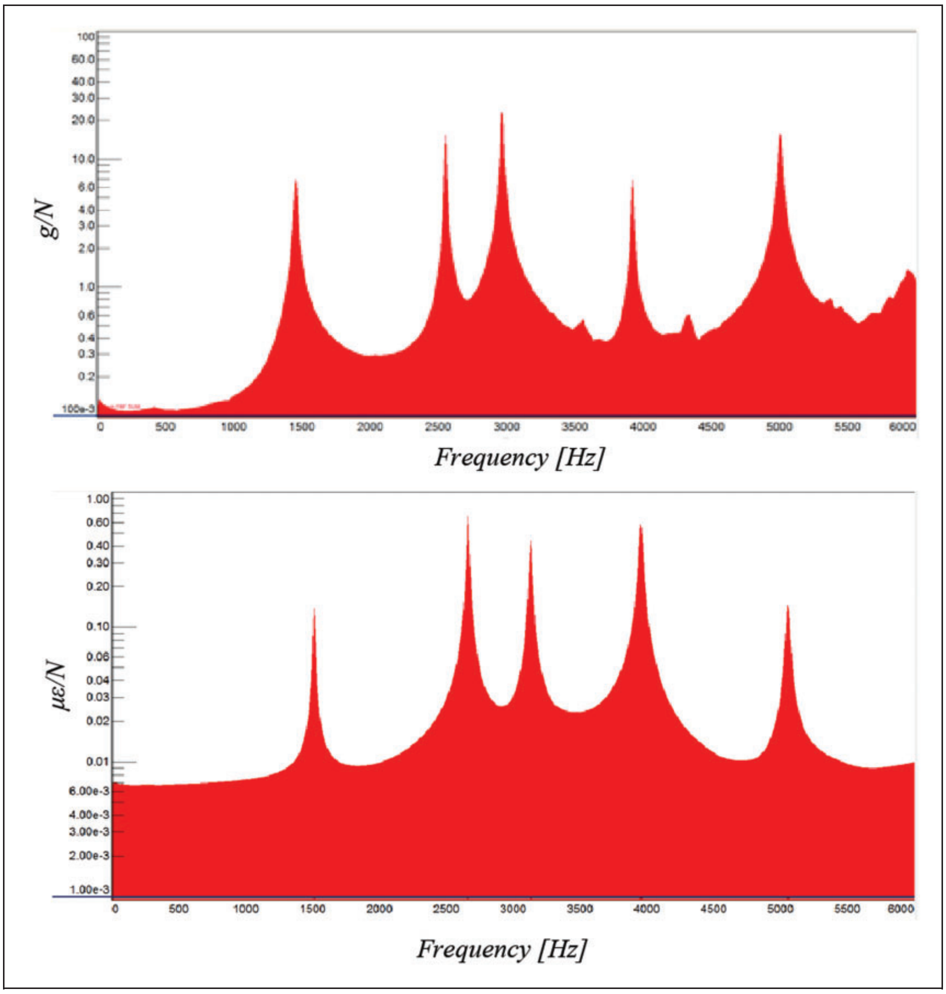


**Figure 4.** Free–free EMA of Bracket A: (a) FRF–sum (amplitude) and (b) SFRF–sum (amplitude).

**Table 3.** MAC values between the free–free EMA of Bracket A with strain sensor in point 1X and with accelerometer in point 1X.

| | | Strain sensor in 1X | | | | |
|---|---|---|---|---|---|---|
| | Fn (Hz) | 1510 | 2661 | 3129 | 3954 | 5053 |
| Accelerometer in 1X | 1452 | 0.98 | | | | |
| | 2551 | 0.01 | 0.83 | | | |
| | 2965 | 0.02 | 0.01 | 0.92 | | |
| | 3921 | 0.06 | 0.04 | 0.01 | 0.86 | |
| | 5004 | 0.02 | 0.05 | 0.04 | 0.01 | 0.76 |

**Table 4.** MAC values between the free–free EMA of Bracket A with strain sensor in point 2Y and with accelerometer in point 1X.

| | | Strain sensor in 2Y | | | | |
|---|---|---|---|---|---|---|
| | Fn[Hz] | 1510 | 2661 | 3129 | 3954 | 5053 |
| Accelerometer in 1X | 1452 | **0.97** | | | | |
| | 2551 | 0.01 | **0.88** | | | |
| | 2965 | 0.01 | 0.01 | **0.82** | | |
| | 3921 | 0.06 | 0.07 | 0.01 | **0.83** | |
| | 5004 | 0.01 | 0.01 | 0.03 | 0.01 | **0.75** |

strain-based data. The experimental campaign has stated that the miniaturised strain sensor can be considered a suitable sensor for modal analysis, leading to precise results if compared with the accelerometer-based modal analysis. Attention has to be paid in the selection of the response location. In particular, as the accelerometer should be located far from nodal line, the strain sensor should be mounted in high deformation zone. The piezoelectric strain sensor avoids the main drawbacks related to strain gauge measurements (e.g. proper calibration, etc.). On the other hand, the main drawback of the piezoelectric strain sensor regards the cost which is rather high (about 500€) if compared to a standard mono-axial accelerometer. Moreover, the strain sensor is a mono-axial strain sensor, while a large variety of tri-axial accelerometers are widespread.

This author believes that in the near future the strain sensor could replace accelerometers for modal parameter estimation in a number of applications, in

**Table 5.** MAC values between the free–free EMA of Bracket B with strain sensor in points 4Y,3Z, 3X and with accelerometer in points 4X,4Y,4Z.

| | | Strain sensor in 4Y, 3Z, 3X | | | | |
|---|---|---|---|---|---|---|
| | Fn (Hz) | 1068 | 1271 | 2229 | 3031 | 3160 |
| Accelerometer in 4X, 4Y, 4Z | 1043 | **0.80** | | | | |
| | 1218 | 0.01 | **0.70** | | | |
| | 2194 | 0.05 | 0.01 | **0.80** | | |
| | 2994 | 0.01 | 0.03 | 0.03 | **0.83** | |
| | 3088 | 0.01 | 0.01 | 0.01 | 0.02 | **0.88** |

**Table 6.** MAC values between the clamped EMA of Bracket B with strain sensor in points 3X and with accelerometer in points 4X, 4Y, 4Z.

| | | Strain sensor in 3X | | | |
|---|---|---|---|---|---|
| | Fn (Hz) | 525 | 760 | 887 | 953 |
| Accelerometer in 4X, 4Y, 4Z | 511 | **0.89** | | | |
| | 738 | 0.01 | **0.88** | | |
| | 886 | 0.38 | 0.02 | **0.71** | |
| | 952 | 0.17 | 0.17 | 0.47 | **0.83** |

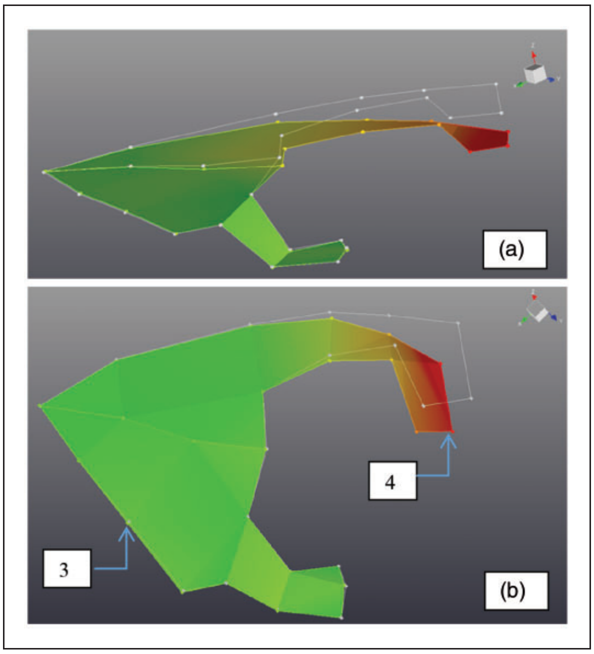


**Figure 5.** First and second mode shape for the clamped EMA of Bracket B at 511 and 738 Hz, respectively. In the first mode (a) the main deformation is in *Z* direction, while for the second mode (b) the main deformation is on the *XY* plane.

particular for operational modal testing in structural systems which must survive severe dynamic loads and for which the strains and stresses are also prime parameters of interest.

**Table 7.** MAC values between the clamped EMA of Bracket B with strain sensor in points 3Z and with accelerometer in points 4X, 4Y, 4Z.

| | | Strain sensor in 3Z | | | |
|---|---|---|---|---|---|
| | Fn (Hz) | 525 | 760 | 887 | 953 |
| Accelerometer in 4X, 4Y, 4Z | 511 | **0.02** | | | |
| | 738 | 0.01 | **0.06** | | |
| | 886 | 0.01 | 0.03 | **0.71** | |
| | 952 | 0.01 | 0.06 | 0.37 | **0.47** |

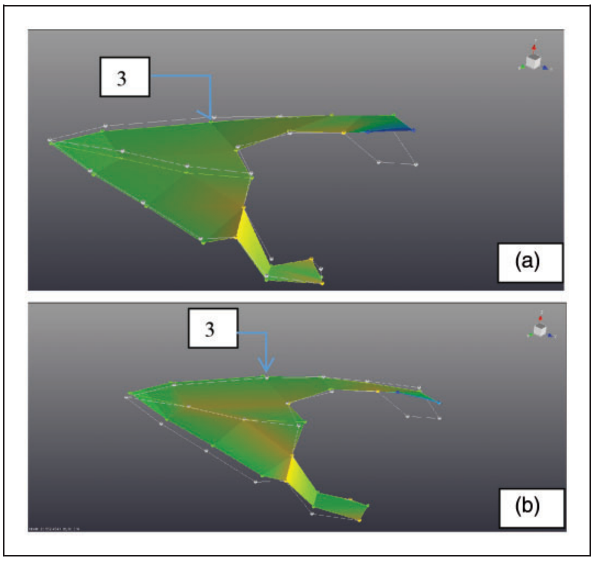


**Figure 6.** Third and fourth mode shape for the clamped EMA of Bracket B at 887 and 953 Hz, respectively.

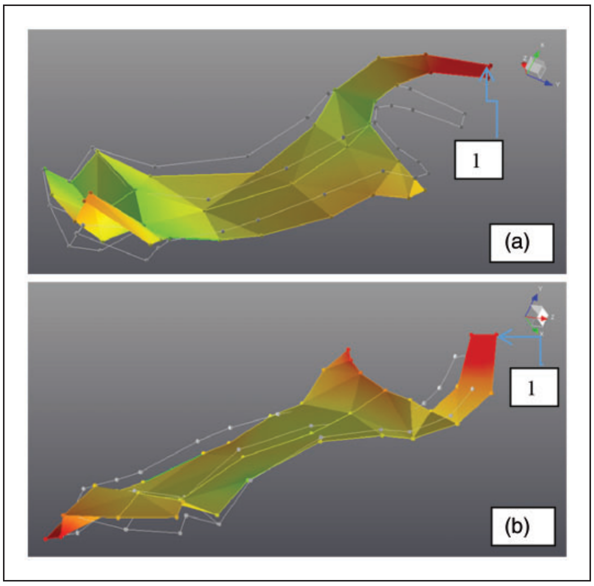


**Figure 7.** First and second mode shape for the free–free EMA of Bracket A at 1452 and 2551 Hz, respectively. The first mode (a) is a torsional mode, while the second mode (b) a torsional/flexural mode.

## Acknowledgments

This work has been developed within the Laboratory of Advanced Mechanics (MechLav) of Ferrara Technopole, realized through the contribution of Regione Emilia Romagna – Assessorato Attivita' Produttive, Sviluppo Economico, Piano telematico – POR-FESR 2007-2013, Attività I.1.1.

## Conflict of interest

The author declared no potential conflicts of interest with respect to the research, authorship, and/or publication of this article.

## Funding

The author received no financial support for the research, authorship, and/or publication of this article.

## References

1. Ewins DJ. *Modal testing: Theory, practice and application*. Taunton: Research Studies Press, 2000.
2. Heylen W, Lammens S and Sas P. *Modal analysis theory and testing*. Belgium: Katholieke Univeriteit Leuven, 2003.
3. Bernasconi O and Ewins DJ. Application of strain modal testing to real structures. In: *Proceedings of 3rd IMAC symposium on computational acoustics*, Cambridge, UK, 1989.
4. Bernasconi O and Ewins DJ. Modal strain/stress fields. *J Modal Anal* 1989; 4: 68–79.
5. Stacker C. Modal analysis efficiency improved via strain frequency response functions. In: *Proceedings of 3rd IMAC symposium on computational acoustics*, Cambridge, UK, 1985.
6. Komrower JM and Pakstys MP. Verification of modal testing and analysis techniques for prediction of dynamic strain in impact loaded structures. In: *Proceedings of 2nd IMAC*, Union College, 1984.
7. Debao L, Hongcheng Z and Bo W. The principle and techniques of experimental strain modal analysis. In: *Proceedings of 7th IMAC*, 1989. 1
8. Hillary B and Ewins DJ. The use of strain gauges in force determination and frequency response function measurement. In: *Proceedings of 2nd IMAC*, Union College, 1984.
9. Song T, Zhang PQ, Feng WQ, et al. The application of the time domain method in strain modal analysis. In: *Proceedings of 4th IMAC*, 1986.
10. Vari LM and Heyns PS. Strain modal testing – A critical appraisal. *R&D J* 1997; 13: 83–90.
11. Yi S, Kong FR and Chang YS. Vibration modal analysis by means of impulse excitation and measurement using strain gauges. In: *Proceedings of IMechE C308/84*, 1984.
12. Rovscek D, Slavic J and Boltezar M. The use of strain sensors in an experimental modal analysis of small and light structures with free-free boundary conditions. *J Vib Control* 2013; 19: 1072–1079.
13. http://www.pcb.com/Literature.aspx
14. Mucchi E. Experimental evaluation of modal damping of automotive components in different boundary conditions. *Meccanica* 2012; 47: 1035–1041.
15. Guillaume P, Verboven P, Vanlanduit S, et al. A poly-reference implementation of the least-square complex frequency-domain estimator. In: *Proceedings of 21st IMAC*, Kissimmee, USA, 2003.